



HAL
open science

Formation of Ni-Nd alloys by Nd(III) electrochemical reduction in molten fluoride

Christophe Nourry, Laurent Massot, Pierre Chamelot, Pierre Taxil

► **To cite this version:**

Christophe Nourry, Laurent Massot, Pierre Chamelot, Pierre Taxil. Formation of Ni-Nd alloys by Nd(III) electrochemical reduction in molten fluoride. *Journal of new materials for electrochemical systems*, 2007, 10 (2), pp.0. hal-03481111

HAL Id: hal-03481111

<https://hal.science/hal-03481111>

Submitted on 15 Dec 2021

HAL is a multi-disciplinary open access archive for the deposit and dissemination of scientific research documents, whether they are published or not. The documents may come from teaching and research institutions in France or abroad, or from public or private research centers.

L'archive ouverte pluridisciplinaire **HAL**, est destinée au dépôt et à la diffusion de documents scientifiques de niveau recherche, publiés ou non, émanant des établissements d'enseignement et de recherche français ou étrangers, des laboratoires publics ou privés.

Formation of Ni-Nd alloys by Nd(III) electrochemical reduction in molten fluoride.

C. Nourry, L. Massot*, P. Chamelot and P. Taxil

Laboratoire de Génie Chimique UMR 5503, Département Procédés Electrochimiques,

Université Paul Sabatier, 31062 Toulouse Cedex9, France

(*) corresponding author:

Massot Laurent

Tel : + 33 (0) 5 61 55 81 94

fax : + 33 (0) 5 61 55 61 39

E-mail : massot@chimie.ups-tlse.fr

Abstract

The electrochemical reduction of Nd(III) in molten LiF-CaF₂ media was investigated on different electrode materials. First, some experiments have been carried out on inert electrode (Ta) and then on a reactive one (Ni). The reduction of Nd(III) on a nickel electrode was observed to lead to intermetallic compounds formation. Metalliding process was carried out on nickel cathode leading formation of the most stable compound in the binary diagram (NdNi₅). Using open-circuit chronopotentiometry and SEM observations, the mechanism of alloys formation and the Gibbs energy of these compounds have been determined for the Nd-Ni system in the 800-950°C range. Finally, reduction of Nd(III) on Cu-Ni electrode has also been studied and the formation of ternary Cu-Ni-Nd alloys, with a high Nd content, was observed.

Key words

Molten fluorides, neodymium, cyclic voltammetry, chronopotentiometry, intermetallic compounds, electrochemistry.

1. INTRODUCTION

During the last twenty years, the interest concerning lanthanides based alloys was increasing significantly due to their interesting properties such as:

- (i) the magnetic properties of Cu-Ni-Ln alloys [1-2];
- (ii) the ductility properties of Al-Ni doped by Nd [3];

(iii) surface properties : the capability of hydrogen adsorption by Ni-Nd alloys can be a pertinent route for hydrogen storage and fuel cells applications [4].

This work is focused on the electrochemical behavior of Nd in the molten LiF-CaF₂ medium in the 800-950°C temperature range, using electrochemical techniques such as cyclic voltammetry and open-circuit chronopotentiometry first on an inert electrode (Ta), then on a reactive electrode (Ni). The cathode was successively an inert material regarding Nd (Ta) then a reactive one (Ni) in order to identify on the cyclic voltammogram and the chronopotentiogram the respective formation of pure Nd and of the Nd-Ni alloys mentioned on the binary diagram [5]. The obtained alloys were observed and characterized by scanning Electron Microscopy coupled with Energy Dispersive Spectroscopy probe. Another technique of preparing these alloys, using a galvanic cell will be examined too. These results allowed characterizing the alloys formation and calculating their Gibbs energies. Those methods are largely described by Taxil *et al* [6]. In the last part, the feasibility of preparing ternary Cu-Ni-Nd alloys using the same methodology was examined by electrochemical reduction of Nd(III) on a Cu-Ni (55-45 at %) cathode material.

2. EXPERIMENTAL

The cell consisted on a glassy carbon crucible (Carbone Lorraine V25) containing the electrolyte bath and introduced in a cylindrical vessel made of refractory steel. The inner part of the vessel was protected against fluoride vapour by a graphite liner. During the experiments, the top of the cell was cooled with water and the cell was placed under argon atmosphere (U grade, less than 5 ppm O₂).

The solvent used as electrolytic bath was the eutectic LiF/CaF₂ (Merck suprapur 99.99%) (77/23 molar percent) and its melting point is 762°C. Before each experiment, the salt mixture was dehydrated by heating under vacuum up to the melting point.

Neodymium trifluoride NdF₃ (Alpha Aesar 99.99%) was used as solute at the 0.1 mol kg⁻¹ concentration. It is introduced into the melt in the form of pellets.

Ta, Ni (1-mm diameter) (Goodfellow 99.95%) and Cu-Ni (55-45 at %) (2-mm diameter) wires were used as working electrodes.

The auxiliary electrode was a glassy carbon rod (Carbone Lorraine V25) with a large surface area (2.5 cm²).

The potentials were referred to a platinum wire (0.5 mm diameter) immersed in the molten electrolyte, acting as a quasi-reference electrode Pt/PtO_x/O²⁻ [7].

All studies of cyclic voltammetry and open-circuit chronopotentiometry were performed using an Autolab PGSTAT30 potentiostat / galvanostat controlled by a computer using the GPES 4.9 software.

After each electrochemical reduction processes, the cathodic products were examined by Scanning Electron Microscopy (LEO 435 VP) and analysed with an EDS probe (Oxford INCA 200) coupled with the SEM device.

3. RESULTS AND DISCUSSION

3.1. Previous results on the NdF₃ reduction mechanism on inert electrode

The reduction mechanism of NdF₃ in LiF-CaF₂ medium was investigated previously on an inert electrode in our laboratory by Hamel *et al.* [8]. It has been proved that the reduction mechanism consists in a single step reduction controlled by diffusion:



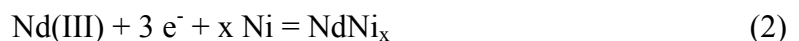
A typical cyclic voltammogram of the system LiF-CaF₂-NdF₃ using Ta electrode is shown in figure 1. The peak at -1.85 V in figure 1 is attributed to Nd(III)/Nd(0) reduction.

3.2. Study of the NdF₃ electrochemical reduction on a reactive electrode

The Ni-Nd system phase diagram shown on figure 2 extracted from ref [5] evidences that neodymium can be alloyed with nickel, giving several intermetallic compounds: Nd₃Ni, Nd₇Ni₃, NdNi, Nd₂Ni, NdNi₃, Nd₂Ni₇ and NdNi₅.

3.2.1 Cyclic voltammetry

Cyclic voltammetry was carried out on a nickel electrode in LiF-CaF₂-NdF₃ (0.1mol.kg⁻¹) system at 800°C. The cyclic voltammogram showed in figure 3, compares the Nd(III) reduction on nickel and on an inert electrode (Ta). In the case of the nickel cathode, we notice reduction waves with high currents at more anodic potentials than the reduction of Nd(III) in pure Nd metal which is observed on the Ta electrode. These waves are attributed to the formation of Ni/Nd alloys by a reaction as below:



Referring to the Nernst law, the lower activity of Nd in the cathodic product explains that the reduction of Nd comes in a Nd intermetallic compound promotes the “depolarization” of the reduction process, so the shift of the electroreduction potential in the anodic sens. Taking into

account the comparison between the voltammograms of fig 1, the depolarization value (ΔE) is estimated at 0.7 V.

3.2.2 Open-circuit chronopotentiometry

Open circuit chronopotentiometry allows to identify all the compounds of the binary Nd-Ni diagram and to calculate their Gibbs energy. The method consists in realizing the pure Nd deposition on the nickel cathode by a short cathodic run and, after the switch off of the current, to measure the potential of this electrode. During the period where the current is off, the intermetallic diffusion of Nd and Ni leads to the successive formation of Nd/Ni compounds, with a decreasing Nd content, at the surface of the cathodic material. The evolution of the surface composition is indicated on the open circuit chronopotentiogram of fig 4 which is typical of the interdiffusion phenomenon leading to the formation of intermetallic compounds, according to ref [9-13]. Each potential plateau of the chronopotentiogram was referred to the potential of Nd, so that it measures the emf of the cell $\text{Nd}_x\text{Ni}/\text{Nd}_y\text{Ni}$, LiFCaF_2 , NdF_3/Nd , associated to the reaction (3).



The emf corresponding to this reaction is:

$$\zeta = \frac{RT}{3(y-x)F} \ln \frac{a_{\text{Nd}(\text{Nd}_y\text{Ni})}^{\text{eq}}}{a_{\text{Nd}(\text{Nd}_x\text{Ni})}^{\text{eq}}} \quad (4)$$

It is possible to calculate the Gibbs energy of this reaction with the following relation:

$$\Delta G = -n F \zeta \quad (5)$$

Where ΔG is the Gibbs energy of the reaction in J mol^{-1} , n is the number of exchanged electrons ($n = 3$), F is the faraday constant.

At the first potential plateau, pure Nd is converted in Nd_yNi . To calculate the Gibbs energy formation of Ni_yNd , ΔG_f , linear combination of ΔG are made ($\Delta G_f = \Sigma \Delta G$), indeed, ΔG_f corresponds to the reaction 6 and it is a linear combination of reactions that occurs on the plateaus (3).



It is possible to calculate step by step the Gibbs formation energy of each intermetallic compound

The values of the Gibbs formation energies obtained for the Ni-Nd system at 800°C, are plotted in figure 5. The most stable compound is the one containing the lowest Nd content, namely NdNi_5 , according to the diagram of fig 2.

3.2.3 Nd/Ni Alloys Gibbs energy between 800 and 920°C

Open-circuit chronopotentiometries were performed at various temperatures (800, 820, 840, 880 and 920 °C) for the Ni-Nd system in order to determine alloys Gibbs energy using § 3.2.2. The results showed on fig 6 concern the solid intermetallic compounds of the binary diagram. Each plotting, related to one compound, exhibits a maximum around 860°C. this maximum should be explained by the α - β neodymium phase transition occurring at the temperature of 863°C [5].

3.2.4 Discussion on the alloys formation

Several runs of electrolysis at constant current were performed on nickel electrodes for alloying the surface of the nickel with neodymium. During these experiment, the potential was controlled to be lower than the one of pure Nd electrodeposition (-1.85V/ref). The cross

section of the cathodes obtained after electrolysis runs was observed by Scanning Electron Microscopy and analysed by E.D.S.

Two operating conditions of electrolysis were used: -35 mA.cm^{-2} at 840°C during 2 hours and -55 mA.cm^{-2} at 840°C during 30 minutes. Typical S.E.M. analyses of these electrodes are shown on figures 7 and 8 respectively. For low currents, and long electrolysis time the layer is composed of a mixing of NdNi_2 and NdNi_3 which have closed stability according to fig 5, while for higher Nd reduction rate, the layer is only composed of NdNi_2 containing the higher neodymium molar ratio to balance the excess of reduced Nd.

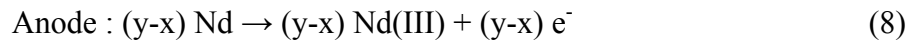
These first results let us assume that:

- Current value and electrolysis time can influence the cathodic product composition
- Short electrolysis at high current allows obtaining alloys with high Nd contents, so NdNi_2 in this work while low currents yield a mixture of alloys with high and low Nd content (here NdNi_2 and NdNi_3)
- The observation of a mixture of NdNi_2 and NdNi_3 (fig 7) while the first phase is changing in the second one should prove that the phase changing is slow
- The overall formation of the alloys is very fast: as we can see on fig 8 the thickness of layers obtained was about $300 \mu\text{m}$ after a two hours electrolysis at 840°C .

3.2.5 Electrodeposition of Nd/Ni alloys on nickel by Metalliding process

The preparation of Nd/Ni alloys can be performed using a galvanic cell associated with the reaction 6. This methodology, called Metalliding, was discovered by Cook in the sixty years [14, 15] and used by our laboratory for the preparation of TaNi [13], NbNi [16] and tantalum

carbide [17]. The current cell provides from to the difference of chemical potential between the two electrode materials, Nd being the anode of the cell, Nd_xNi_y the cathode, with the following electrode reactions:



The reaction process is set up when an electrical contact is realized between the electrodes out of the cell. The scheme of the cell is reported on fig 9. The use of this galvanic cell for obtaining surface alloys has the following advantages:

- To prevent the limitation of the electrode reaction by the diffusion of the ionic specie at the electrode surface
- The preparation of homogeneous alloy layers whatever the geometry of the substrate
- The layer obtained is composed of the most thermodynamically stable compound.

The galvanic cell shown on fig 9 comprises a neodymium foil (Alpha Aesar 99.9% 1 mm thick) as anode and a nickel sheet as cathode, both immersed in the melt at 800°C.

The electrical circuit of the cell was shut during runs of 30, 60, 90 and 120 minutes. After each run, the cathode product was characterised by SEM. The analysis of the alloy layer after the 60 minutes of treatment, reported on figure 10, evidences the formation of a compound of high Nd content at the surface (Nd_2Ni_7) and another layer with a lower Nd content ($NdNi_5$) in contact with the nickel substrate; this observation confirms that the surface reaction leads to the formation of the most stable compound. Similar results were obtained with different experiment duration.

3.3.7 Formation of Cu-Ni-Nd alloys

The formation of Cu-Ni-Nd alloys was investigated using Cu-Ni (55-45 at %) rod (2 mm diameter).

Cyclic voltammetry have been performed on Cu-Ni electrodes. Figure 11 presents a comparison between cyclic voltammogram on inert electrode (Ta) and Cu-Ni. Obviously, the presence of waves at potential more anodic than the neodymium reduction is, once again, due to the formation of alloys or intermetallic compounds. The first wave with a significant current is observed at approximately -1.1V, that corresponds approximately to a similar depolarisation of the Nd(III) reduction compared on inert cathode than this observed on Ni electrode.

Open-circuit chronopotentiometry was performed to confirm the alloys formation. The same technique was used than previously on the nickel electrode case; results are reported in figure 12. The presence of several plateaus confirms that alloys were formed on the electrode surface (cf § 3.2.2). As the Cu-Ni-Nd diagram is not available, it is not possible to identify the compounds corresponding to the plateaus.

A 30 minutes electrolysis run was performed on Cu-Ni electrode at -55 mA cm^{-2} ; the cross sections of the cathode obtained after this run was observed by Scanning Electron Microscopy and analysed with E.D.S. on figure 13. Three intermetallic compounds were observed: $\text{Cu}_{46}\text{Ni}_{37}\text{Nd}_{17}$, $\text{Cu}_{34,5}\text{Ni}_{42,5}\text{Nd}_{23}$ and $\text{Cu}_{26}\text{Ni}_{40}\text{Nd}_{34}$. We can notice in agreement with the case of the nickel substrate: the respective formation at the Cu/Ni interface the phase with the lowest Nd content ($\text{Cu}_{46}\text{Ni}_{37}\text{Nd}_{17}$) which is likely the most stable; at the surface of the electrode, the phase with the highest Nd content, which is supposed to be the least stable phase ($\text{Cu}_{26}\text{Ni}_{40}\text{Nd}_{34}$) and in the middle part of the layer, a compound with an intermediate composition ($\text{Cu}_{34,5}\text{Ni}_{42,5}\text{Nd}_{23}$).

4. CONCLUSION

The electroreduction of neodymium was investigated on Ni electrode in LiF-CaF₂ media.

It has been shown that NdF₃ can be reduced on reactive electrode to form compounds with the electrode substrate. Identification of the compounds produced by this reaction and calculation of their Gibbs energy were carried out using the open circuit chronopotentiometry while S.E.M. observation and E.D.S. analysis allow the alloy layer at the cathode surface to be characterised after electrolysis.

The influence of the temperature in the 800-900°C range on the Gibbs energy of the Ni-Nd compounds was also studied. Similar experiments with a Cu-Ni cathode lead to ternary compounds of the Cu-Ni-Nd system. These results open promising routes for preparing based lanthanides alloys with relevant mechanic or magnetic properties.

ACKNOWLEDGMENTS

The authors express their thanks to the GDR RSF Thorium and PCR Paris from the PACE program for financial support for this work.

References

- [1] E. Burzo, T. Crainic, M. Neumann, L. Chioncel, C. Lazar; *J. Magn. and Magn. Mat.* 209-291, 2005, 371-373.
- [2] A.G. Kuchin, A.S. Ermolenko, Yu.A. Kulikov, V.I. Khrabrov, E.V. Rosenfeld, G.M. Makarova, T.P. Lapina, Ye.V. Belozerov; *J. Magn. Magn. Mater.* In press 2005.
- [3] C.Y. Chung, C.Y. Kie and T.Y. Hsu; *Scripta Materialia*, 37, 1, 99-102, 1997.
- [4] G. Jin, H. Li; *J. Phy. And Chem. of Solids*; 62 (2001) 2055-2058.
- [5] *Binary Alloy Phase Diagrams*, Second Edition ASM International, (1996).
- [6] P. Taxil, P. Chamelot, L. Massot and C. Hamel, *J. Min. Mett.*, 39 (1-2) B (2003) 177-200
- [7] Berghoute Y., Salmi A., and Lantelme F., *J.Electroanal.Chem.*, 365 (1994) 171-178.
- [8] C. Hamel, P.Chamelot, P. Taxil, *Electrochimica Acta* 49 (2004) 4467-4476.
- [9] W. Weppner, R.A. Huggins, *J Electrochem.Soc.*, 124 (1977) 1569
- [10] W. Weppner, R.A. Huggins, *J Electrochem.Soc.*, 125 (1978) 5
- [11] G.S. Picard, Y.E. Mottot, B.L. Trémillon, *Proc. of the 4th internat. Symp. On Molten Salts*, Electrochemical Society Symposium, San Francisco, May 1983
- [12] P. Taxil, Thesis, Toulouse 1985
- [13] P. Taxil, *J. Less Comm. Metals*, 113 (1985) 89
- [14] Cook N.C., *Sci American*, 221(2) (1969) 38.
- [15] Cook N.C., US Patent 2970 091 (1961); 3 024 176 (1962); 3 024 177 (1962); 3 232 863 (1966).
- [16] Taxil P. and Qiahozi Y., *J.App. Electrochem.*, 15(6) 1984 (947-52).
- [17] Massot L., Phd Thesis Toulouse 2002 France.

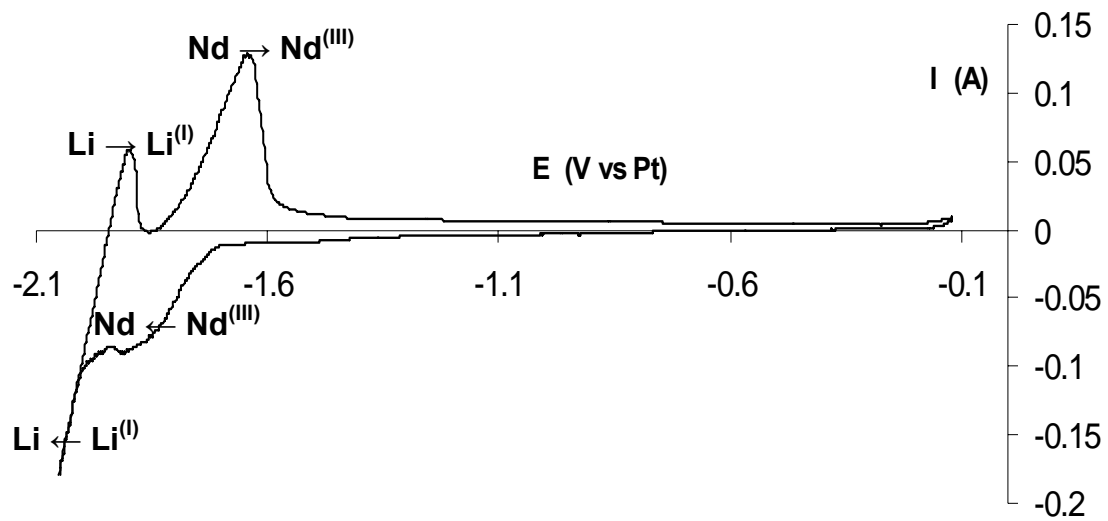


Figure 1

Cyclic voltammogram in $\text{LiF-CaF}_2\text{-NdF}_3$ ($0,1 \text{ mol.Kg}^{-1}$) at 800°C scan rate: 100mv s^{-1} .

Working Electrode: Ta ($S = 0.315 \text{ cm}^2$) ; Auxiliary Electrode.: vitreous carbon ; Quasi-reference EL. : Pt.

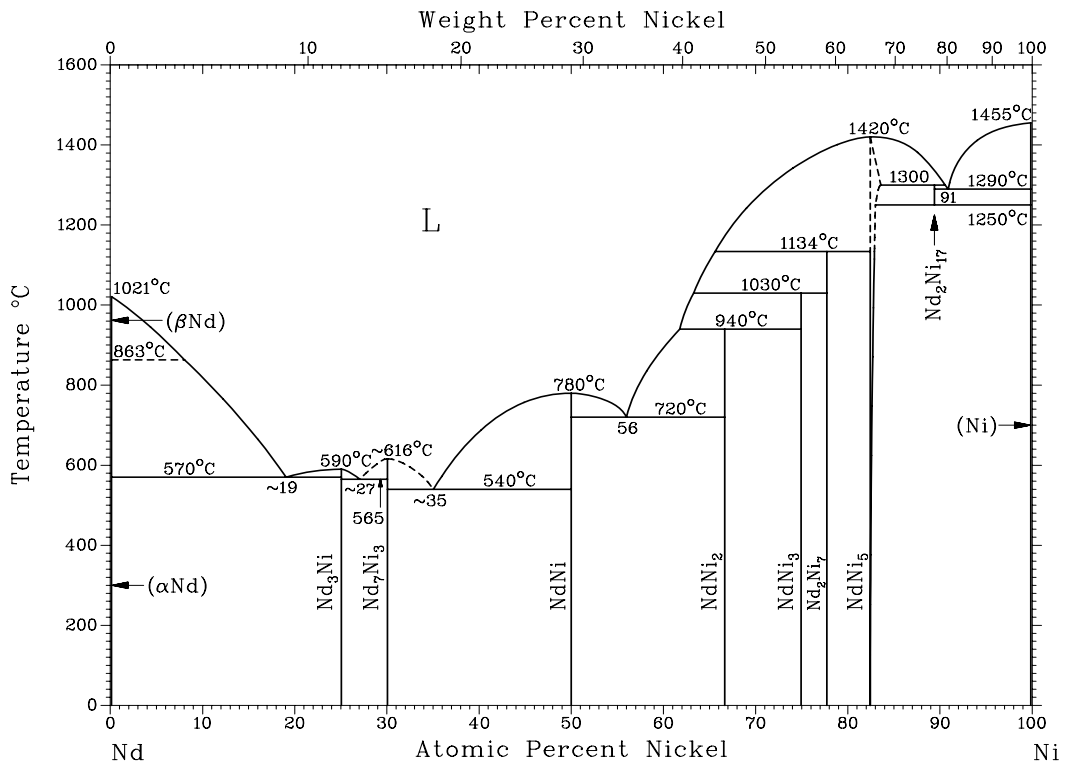


Figure 2

Nickel – Neodymium phase diagram from ASM binary alloys phase diagrams database [5].

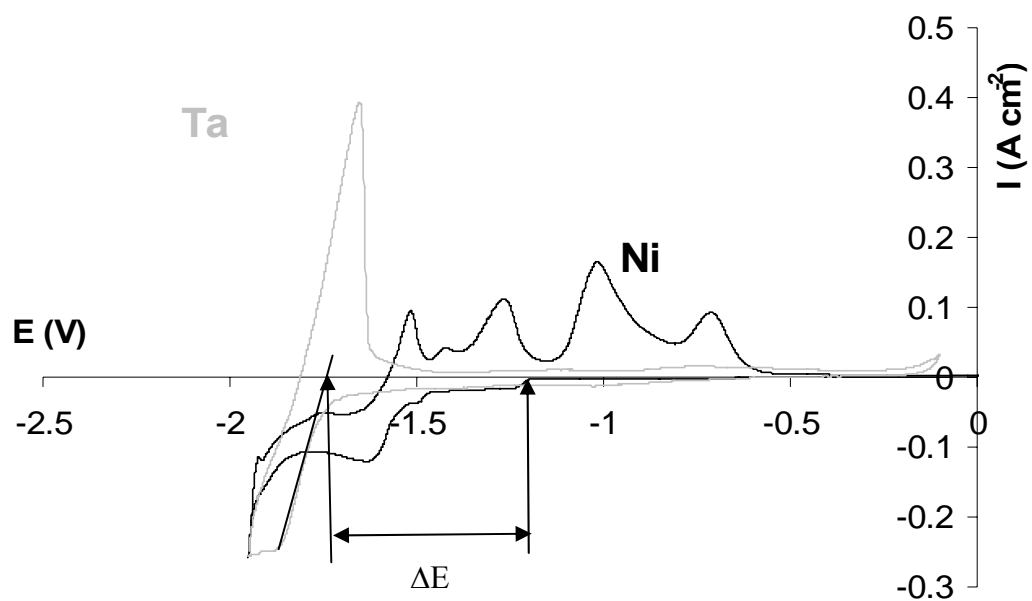


Figure 3

Comparison of the cyclic voltammograms of the LiF-CaF₂-NdF₃ (0,1 mol.Kg-1) system on tantalum and nickel electrodes at 100 mV/s and T = 800°C. Auxiliary Electrode.: vitreous carbon ; Quasi-reference Electrode : Pt.

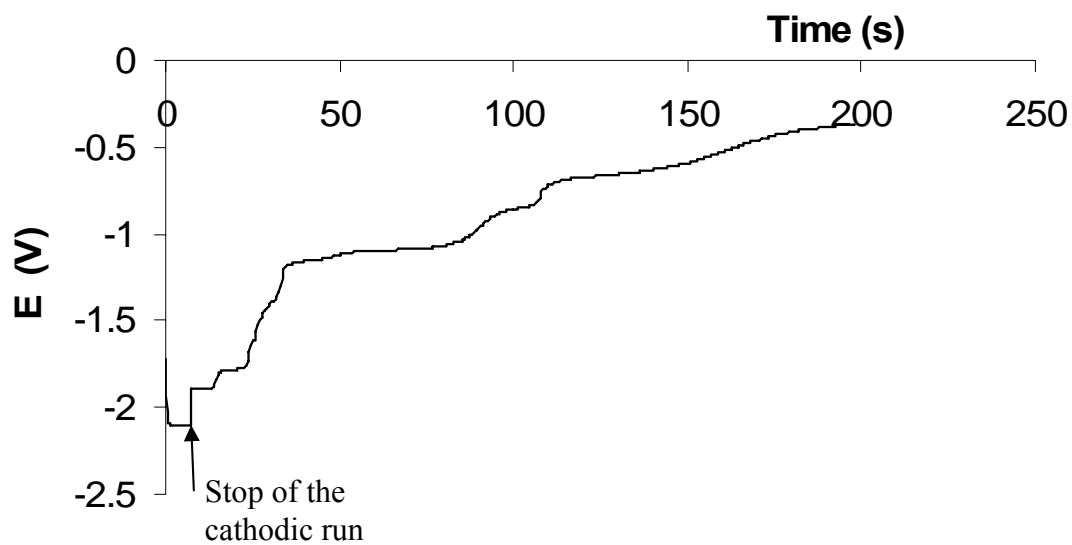


Figure 4

Open-circuit chronopotentiogram of the $\text{LiF-CaF}_2\text{-NdF}_3$ ($0,1 \text{ mol.Kg}^{-1}$) system on nickel electrode at $T = 800^\circ\text{C}$. Auxiliary Electrode: vitreous carbon ; Quasi-reference Electrode: Pt.

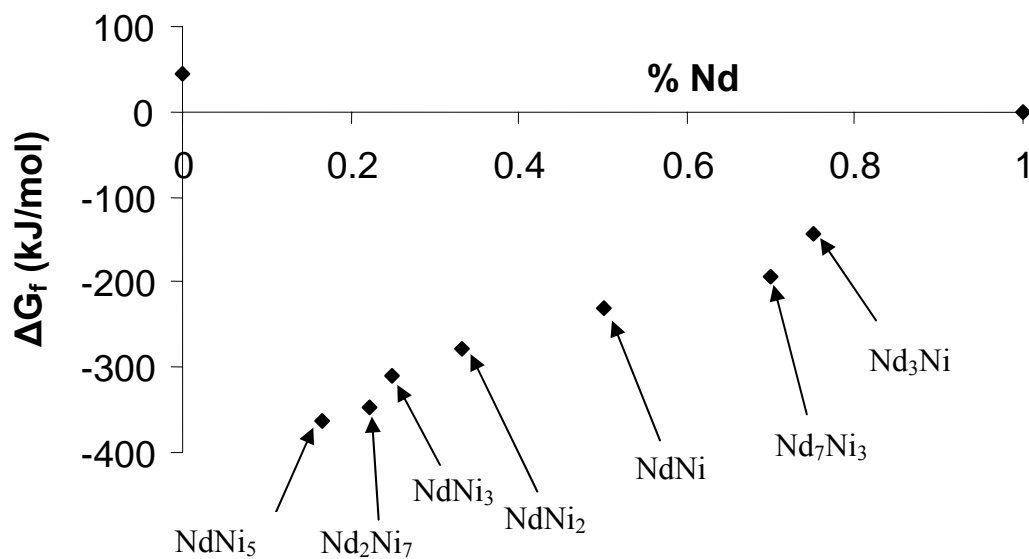


Figure 5

Calculated Gibbs energy of the Ni-Nd intermetallic compounds at 800°C , according to the § 3.2.2.

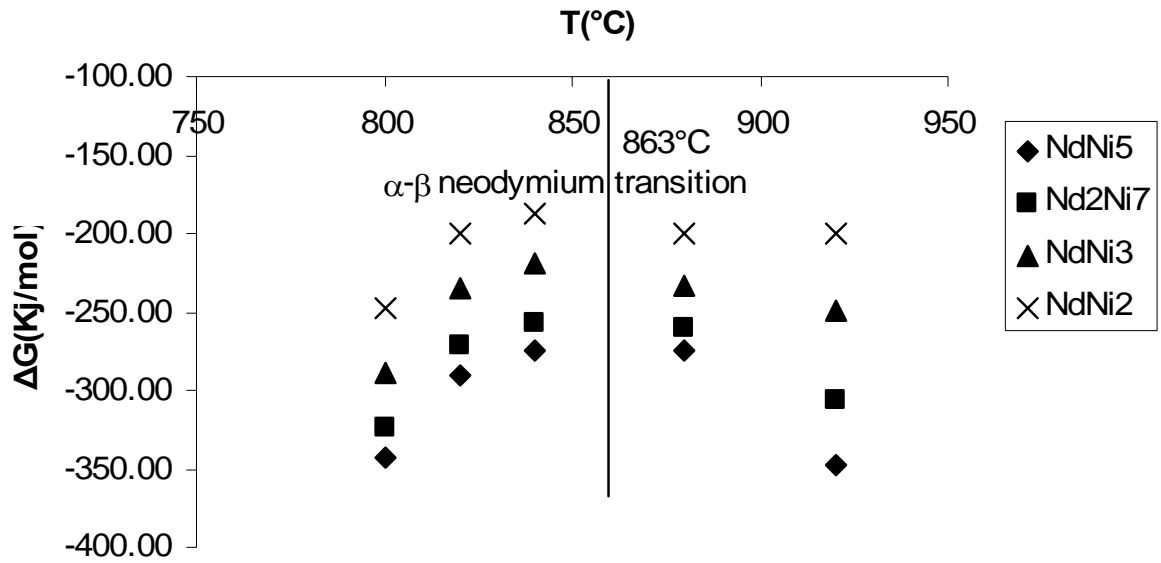


Figure 6

Calculated Gibbs energy for Ni-Nd intermetallic compounds solid between 800 and 920°C.

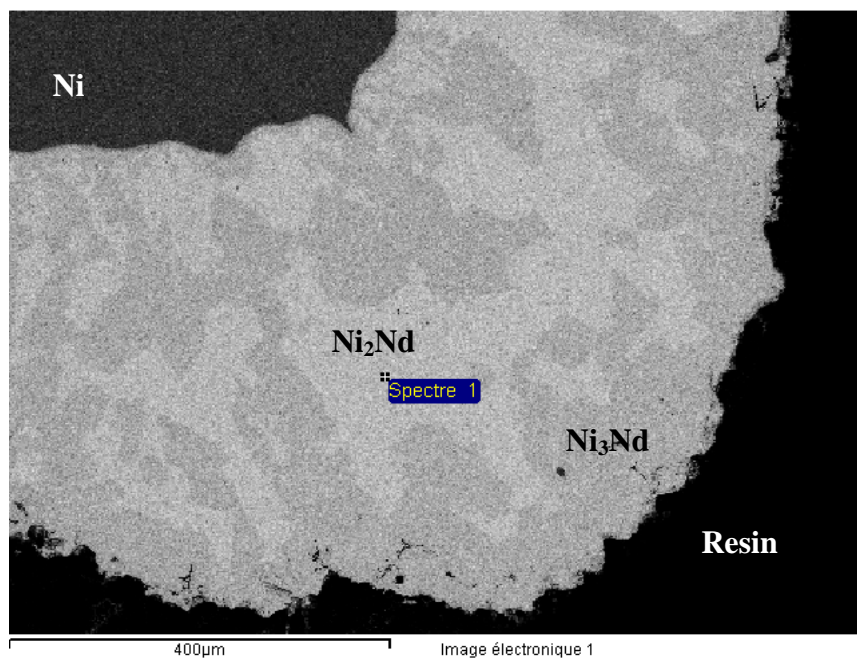


Figure 7

SEM micrograph of the cross section of a nickel sheet after reduction of NdF_3 at $-35 \text{ mA}\cdot\text{cm}^{-2}$ at 840°C for 2 hours.

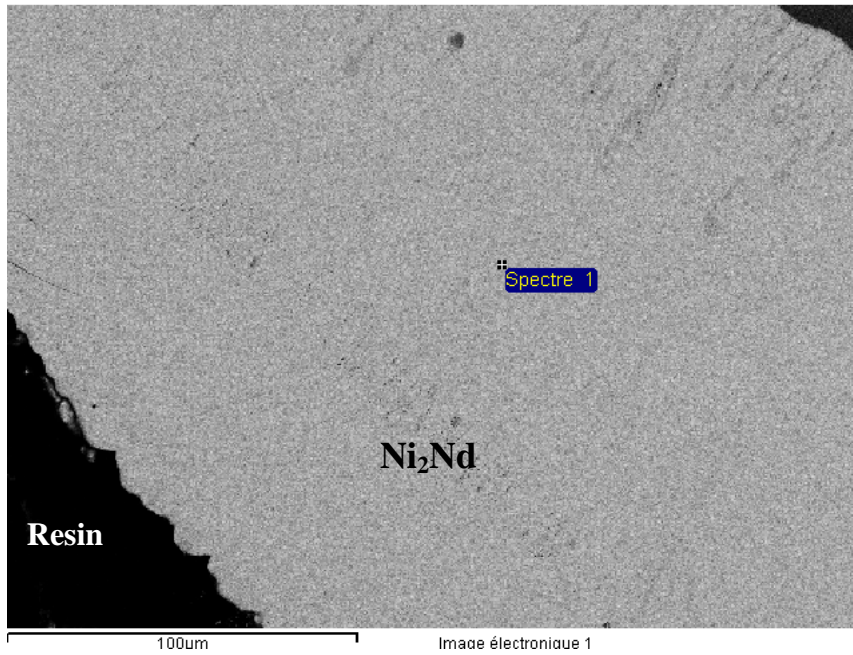


Figure 8

SEM micrograph of the cross section of a nickel sheet after reduction of NdF_3 at $-55 \text{ mA}\cdot\text{cm}^{-2}$ at 840°C for 30 minutes.

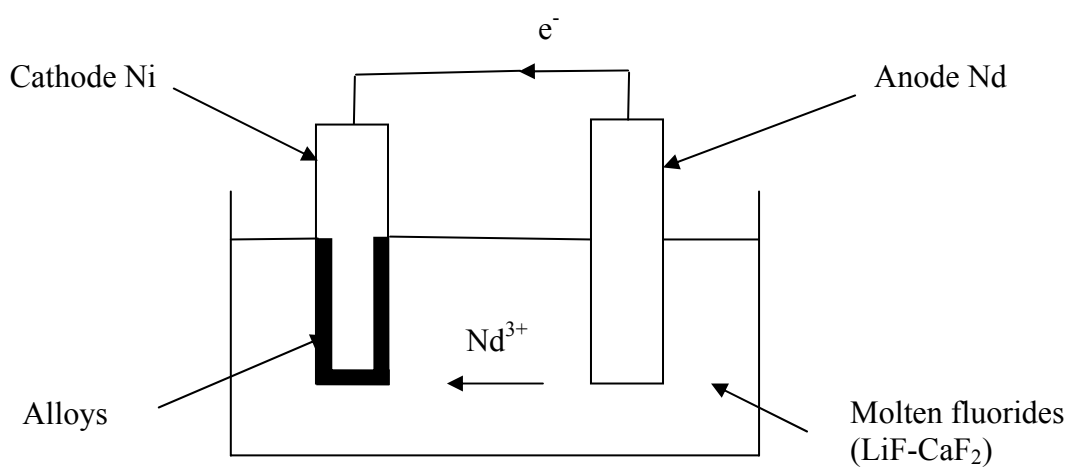


Figure 9

Scheme of the galvanic cell used for the Metalliding process.

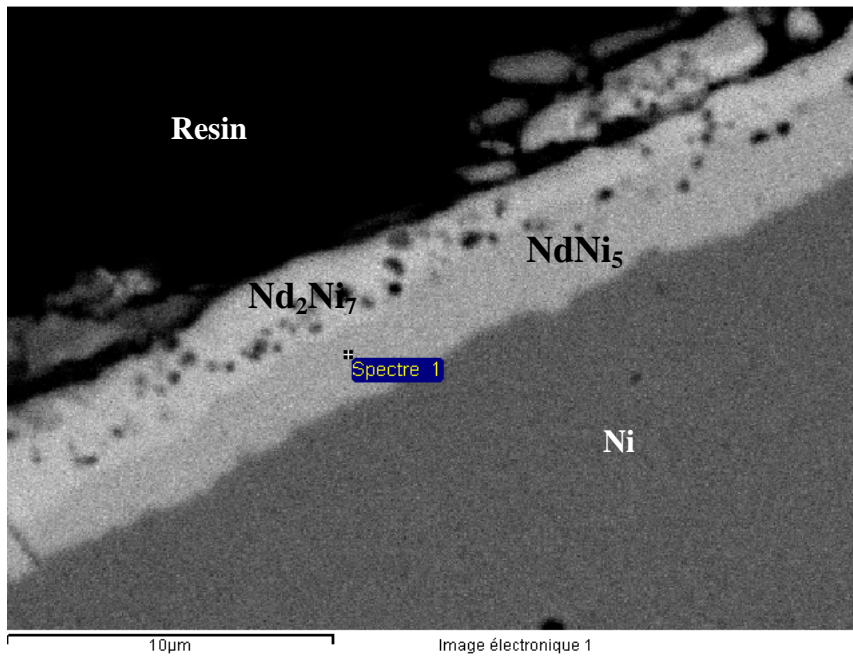


Figure 10

SEM micrograph of the cross section of a nickel sheet after a 1 hour metallizing.

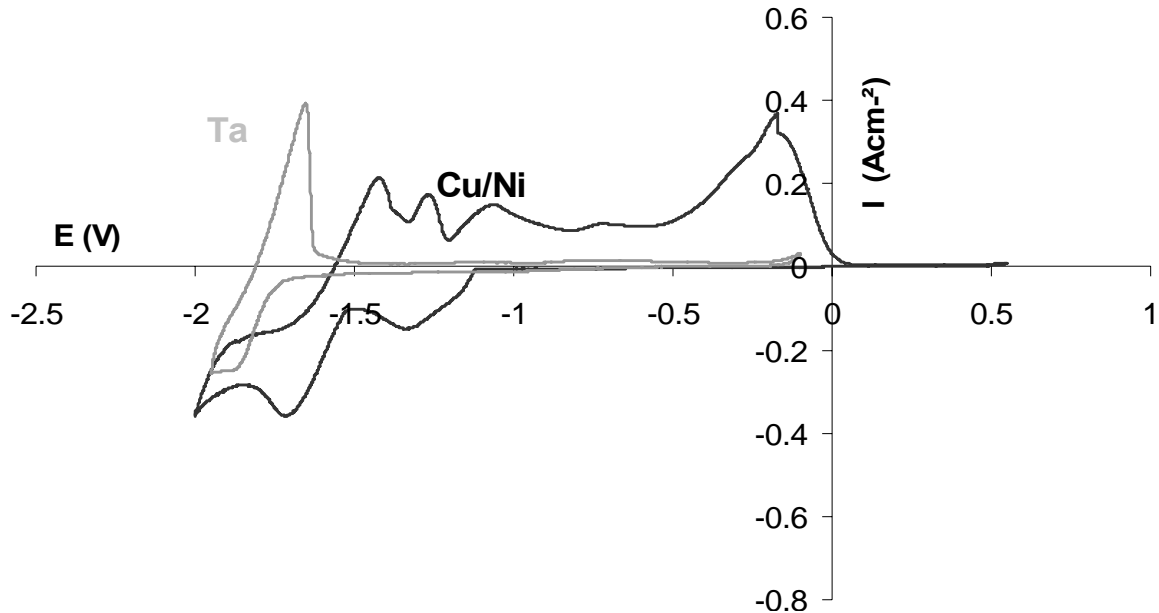


Figure 11

Comparison of the cyclic voltammograms of the $\text{LiF-CaF}_2\text{-NdF}_3$ ($0,1 \text{ mol.Kg}^{-1}$) system on tantalum and copper-nickel (55-45 at %) electrodes at 100 mV/s and $T = 800^\circ\text{C}$. Auxiliary Electrode: vitreous carbon ; Quasi-reference Electrode: Pt.

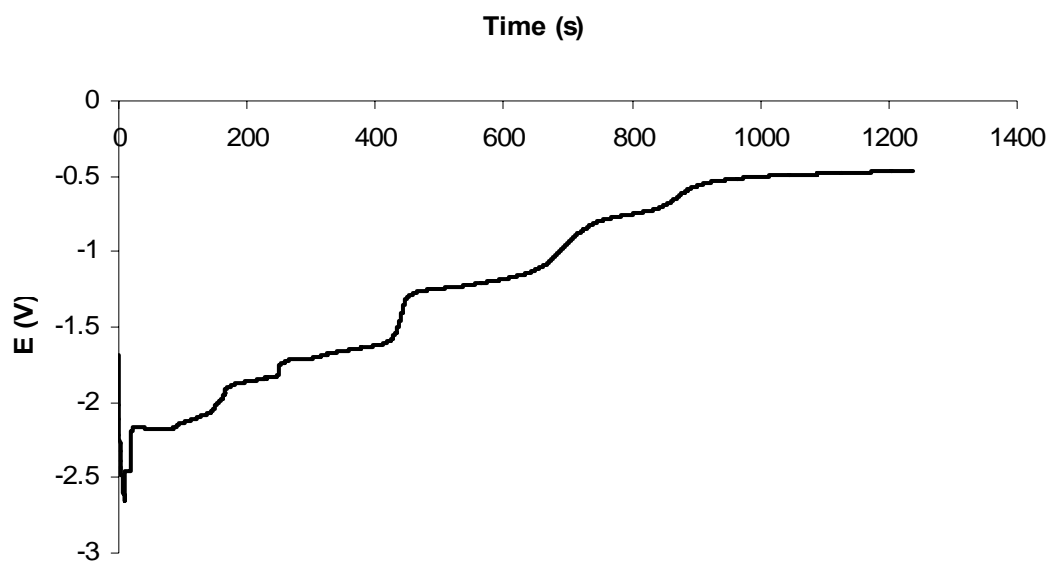


Figure 12

Open-circuit chronopotentiogram of the $\text{LiF-CaF}_2\text{-NdF}_3$ ($0,1 \text{ mol.Kg}^{-1}$) system on copper-nickel (55-45 at %) electrode at $T = 800^\circ\text{C}$. Auxiliary Electrode: vitreous carbon ; Quasi-reference Electrode: Pt.

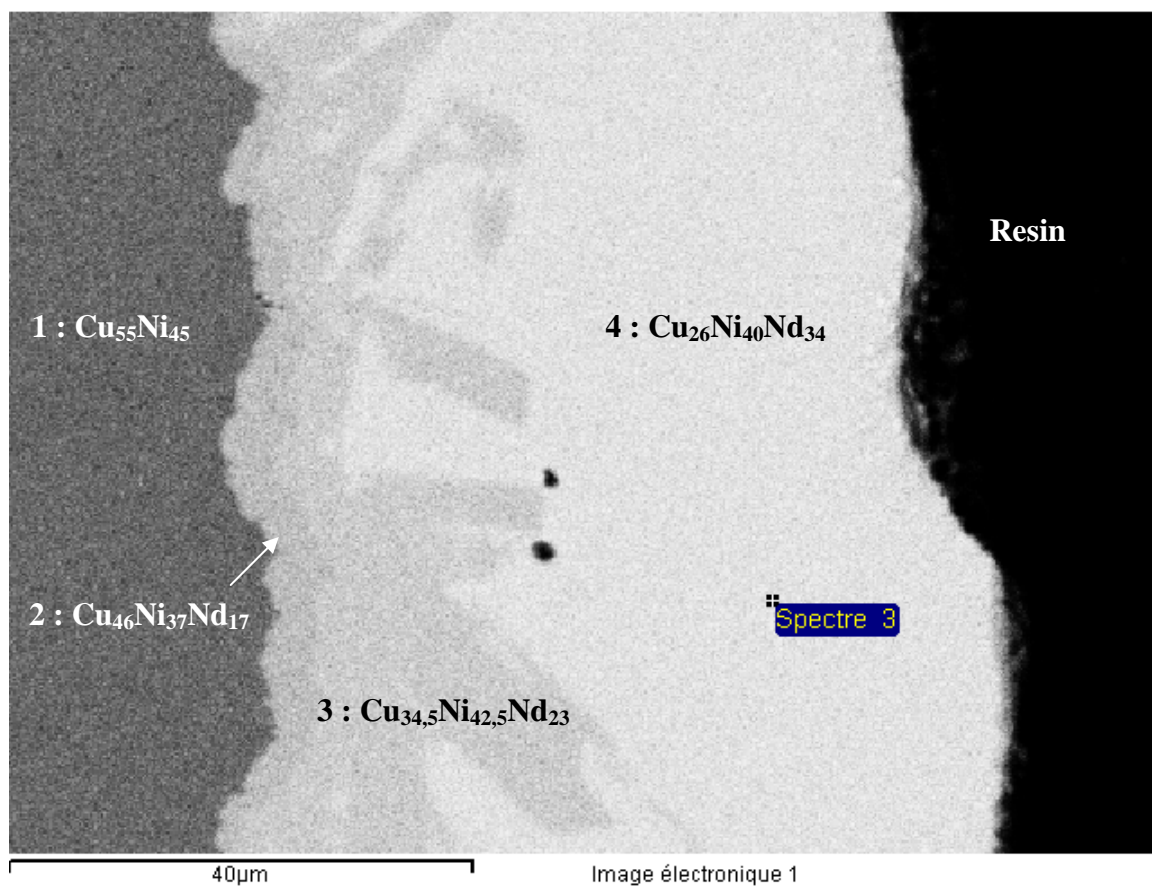


Figure 13

SEM micrograph of the cross section of a copper-nickel (55-45 at %) electrode after reduction of NdF_3 at $-55 \text{ mA}\cdot\text{cm}^{-2}$ at 840°C for 30 minutes.